NASA
TP
2161
c.1

TECH LIBRARY KAFB, NM
0067717

NASA
Technical
Paper
2161

April 1983

Solid Spherical Glass Particle Impingement Studies of Plastic Materials

LOAN COPY: RETURN TO
AFWL TECHNICAL LIBRARY
KIRTLAND AFB, N.M.

P. Veerabhadra Rao,
Stanley G. Young,
and Donald H. Buckley

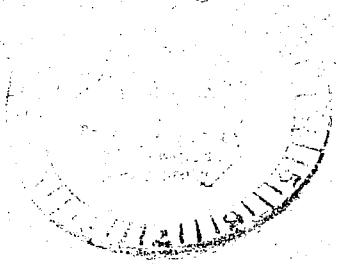

NASA

25th Anniversary
1958-1983

TECH LIBRARY KAFB, NM
0067717

NASA
Technical
Paper
2161

1983

Solid Spherical Glass Particle Impingement Studies of Plastic Materials

P. Veerabhadra Rao,
Stanley G. Young,
and Donald H. Buckley
Lewis Research Center
Cleveland, Ohio

NASA
National Aeronautics
and Space Administration

**Scientific and Technical
Information Branch**

Summary

Optical and scanning electron microscope studies were conducted to characterize the erosion resistances of polymethyl methalcrylate (PMMA), polycarbonate, and polytetrafluoroethylene (PTFE). Erosion was caused by a jet of spherical glass beads at normal impact. During the initial stages of damage, the surfaces of these materials were studied using a profilometer. Material buildup above the original surface was observed on polycarbonate and PMMA. As testing progressed, this buildup disappeared as the erosion pit became deeper. Little or no buildup was observed on PTFE. PTFE is the most resistant material and PMMA the least. At early stages of damage and at low-impact pressures, material removal mechanisms appear to be similar to those for metallic materials. The flake-like debris observed on the surface, which is indicative of deformation wear by repeated impact and eventual fatigue, caused material loss. At higher impact pressures, evidence of surface melting was noted, and it is believed to be the result of heat generated by impact.

Introduction

The damage and erosion caused by the impact of solid particles on the surfaces of aircraft engine components (refs. 1 to 5), helicopter blades (ref. 6), rocket motor nozzles (ref. 7), missiles (ref. 5), Earth satellites (ref. 8), and space vehicles (ref. 9) have received increased attention in recent years. In addition to metallic materials, nonmetallic materials are being used in increasing amounts in structures as well as for viewing screens, windows, and metallic surface protection. Some deleterious effects of erosion on nometallic surfaces are the loss of visibility, degradation of electromagnetic properties, and interference with communications as well as material damage and loss. Material degradation can occur during operation of tactical aircraft during severe weather (e.g., dust and sand storms). Solid impingement erosion is also of vital interest in defense applications such as in optically guided missiles, for laminated plastic transparent windshields, and for canopies (ref. 10).

Many studies on the erosion of ceramic materials and glasses due to single and multiple solid particle impact are reviewed in the literature (refs. 9 to 11). However, a limited number of studies have concentrated on the erosion characteristics and resistance of polymeric, elastomeric, and plastic bulk materials (refs. 2, 3, 7, and 12 to 19) and coatings (refs. 7, 18, and 20). In the various studies, the type of device, erodent particle shape and size, impingement velocity, angle of incidence, etc., have been changed. Normal impingement studies of various plastic materials are mentioned here. Thus, epoxy resin (refs. 2 and 15), nylon (refs. 2, 14, 15, and 17), polypropylene (refs. 3, 14, and 15), Tufnol (ref. 7), perspex (refs. 7 and 13), and polyurethane (ref. 15) have been tested. On the other hand, polyurethane and fluorocarbon (refs. 18 and 20) coatings have been tried to investigate their resistance during solid particle impingement. Solid impingement erosion of bulk plastic materials has received little emphasis (ref. 10). However, in view of their widespread use as coatings for aircraft radomes, antenna covers, and external skin protection, there are many instances of damage and erosion in real situations (refs. 6 and 20).

This work studies the erosion of three commonly known plastic materials (polymethyl methacrylate (PMMA), polycarbonate, and polytetrafluoroethylene (PTFE)) using spherical glass bead erodent particles at normal incidence to gain insights into the surface transformations and morphology. Possible erosion mechanisms are discussed, based on surface analyses by optical and scanning electron microscopy and surface profilometry.

Materials, Apparatus, and Procedure

Materials

Specimen materials were polymethyl methacrylate (PMMA), polycarbonate, and polytetrafluoroethylene (PTFE). The mechanical and other properties of these three thermoplastic materials are presented in table I (ref. 21). The specimens, which were 25 millimeters wide, 37 millimeters long, and 6.4 millimeters thick, were cleaned with alcohol and dried with compressed air.

Apparatus and Experimental Procedure

The investigations in this report were conducted with a commercial sandblasting facility. Test specimens of plastic materials were eroded by normal incidence of high velocity, commercial grade number 9 spherical glass bead particles (average diameter, $\sim 20\ \mu m$; standard deviation, $12\ \mu m$). The glass bead particle distribution is shown in figure 1. Figure 2 shows a SEM energy dispersive X-ray spectrograph of the glass beads. Table I presents the properties of glass which are similar to the composition of the glass beads used in this study.

A schematic diagram of the steady-jet-impingement apparatus is shown in figure 3. The distance between the specimen and the nozzle (diameter, 1.18 mm) was 13 millimeters. Argon was used as the driving gas at a 0.27-megapascal (gage) pressure. The average particle velocity was 72 meters per second. The glass bead flow at this pressure was approximately 0.98 gram per second.

Before exposure all specimens were cleaned with distilled water and alcohol. The materials were tested in the as-received condition. The original surface roughness

TABLE I. - MECHANICAL AND OTHER PROPERTIES OF TEST MATERIALS

Properties	Methyl-methacrylate (PMMA) (a)	Poly-carbonates (a)	Polytetra-fluoro-ethylene (PTFE) (a)	Alumino-silicate glass (b)
Modulus of elasticity, MPa	2380 to 3400	1975 to 2210	224 to 442	77340
Tensile strength, MPa	48 to 75	54 to 65	14 to 31	----------
Ultimate resilience,[c] MN-m/m^3	0.48 to 0.83	0.74 to 0.9	0.44 to 1.09	----------
Ultimate elongation, percent	2 to 10	20 to 100	200 to 400	----------
Yield stress, MPa	----------	54 to 68	11 to 14	----------
Strain energy,[d] MN-m/m^3	----------	11 to 65	25 to 90	----------
Yield strain, percent	----------	----------	50 to 70	----------
Rockwell hardness	M80 to M105	M70 to M180	D50 to D65	----------
Notched Izod impact strength, J	0.41 to 0.81	10.85 to 21.70	3.39 to 8.14	----------
Specific gravity	1.18 to 1.2	1.2	2.1 to 2.3	2.5
Heat distortion at 1.8 MPa, °C	66 to 99	135 to 145	60	----------
Specific heat, cal/g	0.35	0.3	0.25	----------
Linear thermal expansion coefficient, °C	5×10^{-5} to 9×10^{-5}	6.6×10^{-5}	10×10^{-5}	0.5×10^{-6}
Maximum continuous service temperature, °C	60 to 93	138 to 143	260	[e]1210
Refractive index	1.48 to 1.5	1.6	----------	1.5 to 1.55
Softening point, °C	----------	----------	----------	955

[a]Ref. 21.
[b]Kimble Glasses Technical Data, Owens-Illinois.
[c]Defined as (tensile strength)^2/(2 x modulus of elasticity).
[d]When the stress-strain curves are not available, strain energy can be approximated as elongation x ((yield stress + tensile strength)/2).
[e]Working point.

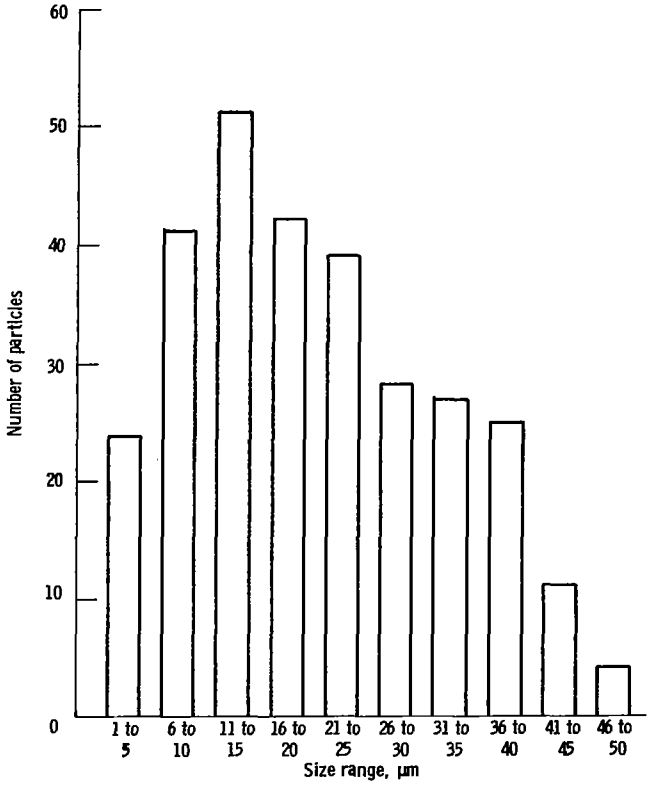

Figure 1. - Particle size distribution of glass beads.

was 0.53 micrometer CLA for the PMMA and polycarbonate and 2.06 micrometers CLA for PTFE. Specimens were weighed before and after each exposure to the impinging jet of glass beads, and weight loss values were converted to volume loss by dividing by density. Traces of the eroded surfaces were recorded with a profilometer, and the eroded surfaces were observed and photographed with light optical and scanning electron microscopes. The specimens that were prepared for SEM examination were gold sputter-coated in order to make them conductive.

Results and Discussion

Erosion Progress and Morphology

The effects of glass bead impingement on PMMA and polycarbonate during the initial phases of erosion (from 3 to 60 sec) are shown in figures 4 and 5, respectively. Figure 6 presents SEM micrographs of erosion on PTFE as functions of time from 1 to 15 minutes.

Separate specimens were tested for each exposure time shown in these figures in order to eliminate the effects of interrupted tests. The apparent reduction in the damage area with respect to exposure time, as observed in some cases in figures 4 and 5, are artifacts due to difficulties in

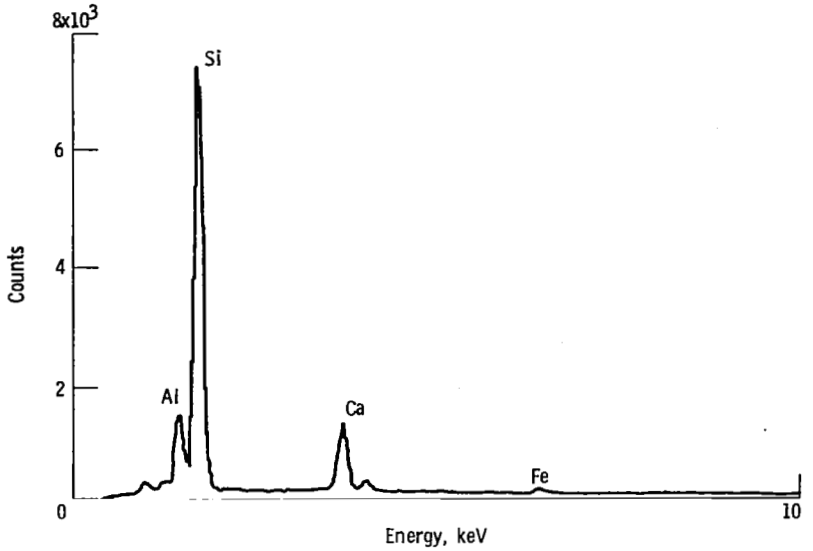

Figure 2. - EDS analysis of glass beads.

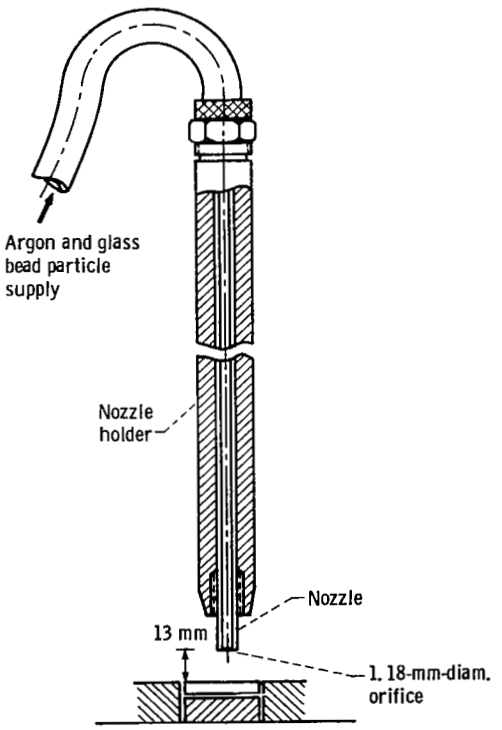

Figure 3. - Schematic diagram of nozzle holder arrangement for impingement apparatus at normal incidence.

focussing all areas of the pit with an optical microscope. Surface profiles at selected erosion intervals for these materials are shown in figures 7 to 9.

The damage pattern may be divided into four regions (indicated in figs. 7 and 8). Region 1 is a central irregular pit surrounded by region 2, a nonuniform buildup of plastic material and glass. Region 2 consists of peaks and valleys from 30 to 100 micrometers deep. Region 3 is a slightly raised region which slopes toward the original surface. Region 4 is a depressed area 5 to 10 micrometers below the original surface level.

Evidence for material buildup can be seen in the surface traces of PMMA and polycarbonate (figs. 7 and 8). These are believed to be due to heat distorsion or partial melting and redeposition of material during impingement. A temperature rise as high as 190° C during impact conditions has been reported (ref. 7). Also, increased levels of the glass bead material are observed in this area. Material buildup was negligible for PTFE (fig. 9). However, the surfaces of the PTFE specimens were observed to have changed color (from white to light brown) after glass bead impact. This color change is also believed to be due to the heat generated during impingement. It is reasonable that PTFE would be most affected by heat in view of its lower heat distortion temperature (table I). Darkening of nylon and polypropylene surfaces due to solid impingement (ref. 14) has been attributed to a chemical change to the surface possibly associated with localized heating. Figure 10 shows SEM micrographs of an eroded PMMA specimen exposed to glass bead impingement for 15 seconds (the same as the surface profile in fig. 7(c)). These micrographs show material buildup, a fissure between regions 2 and 3 (fig. 10(a)), and layers or bands in some areas (fig. 10(b)). These bands are, in general, circumferential arcs surrounding the center of impact with decreasing elevations away from the center of impact. They are believed to be formed by melting and resolidification of the plastic material. However, further studies are necessary to identify the mechanism(s) involved with the formation of these stratified layers.

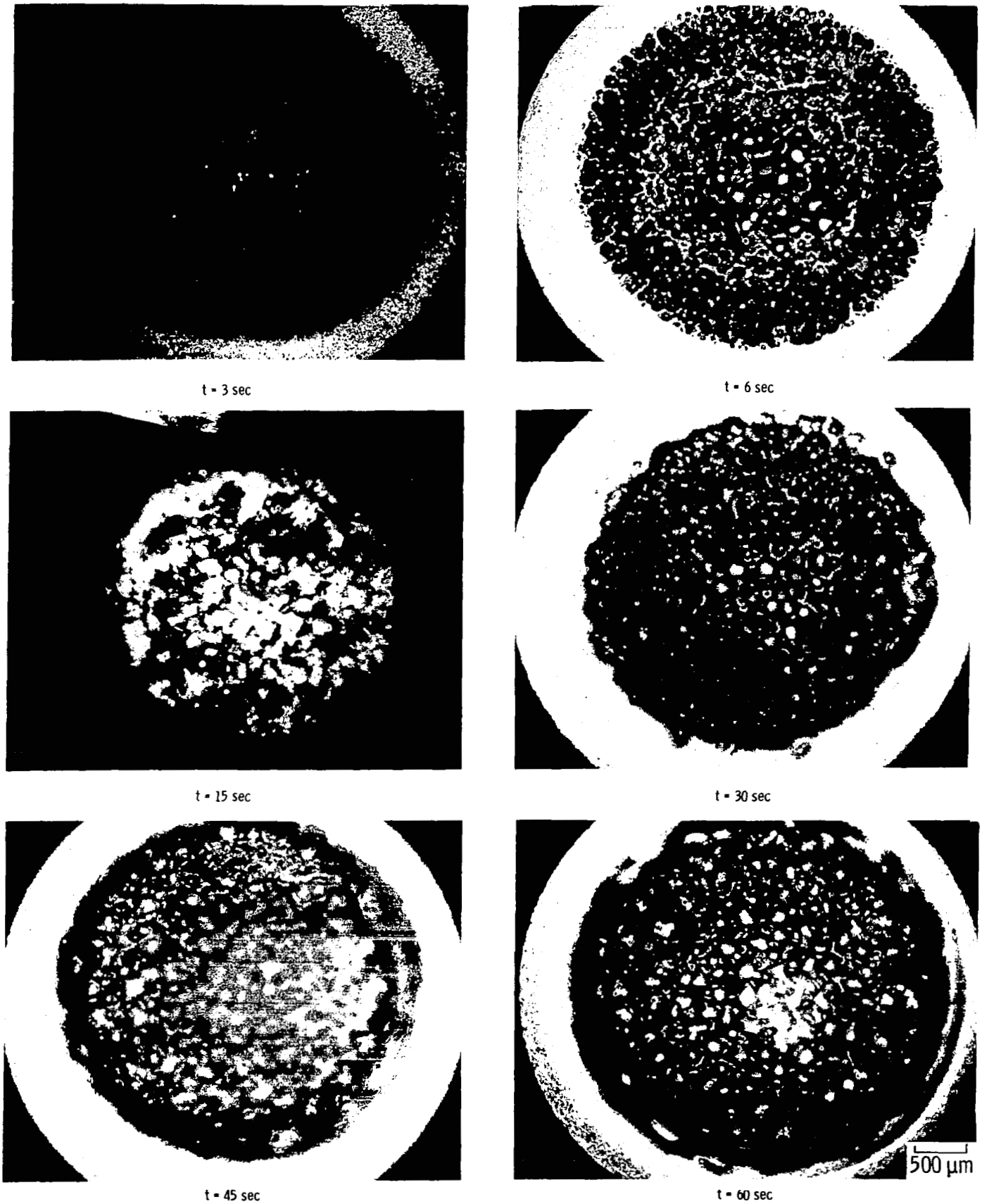

Figure 4. - Photomicrographs of PMMA surfaces exposed to glass bead impingement at 0.27-megapascal gas pressure as function of time.

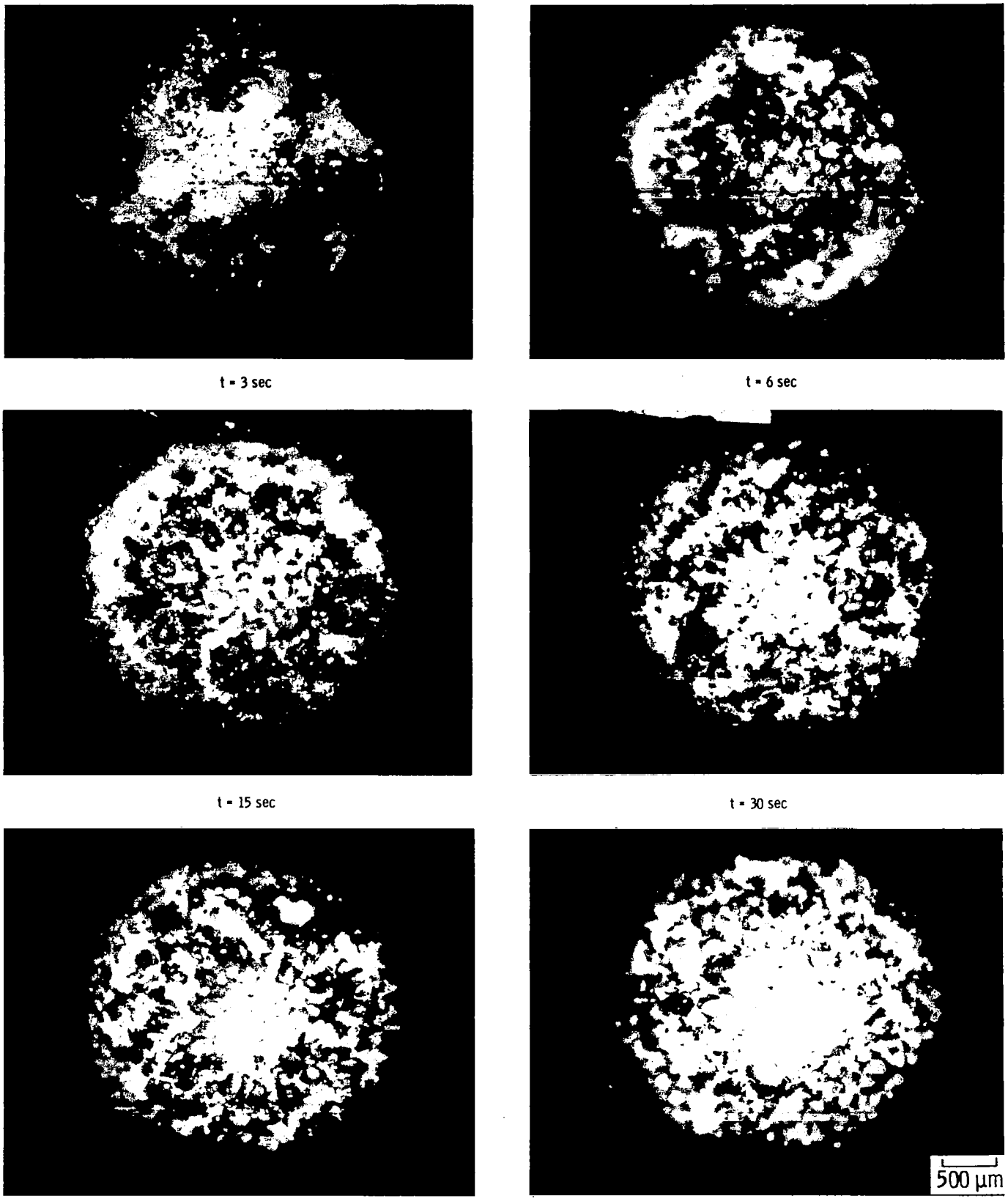

Figure 5. - Photomicrographs of polycarbonate surfaces exposed to glass bead impingement at 0.27-megapascal gas pressure as function of time.

t = 1 min

t = 2 min

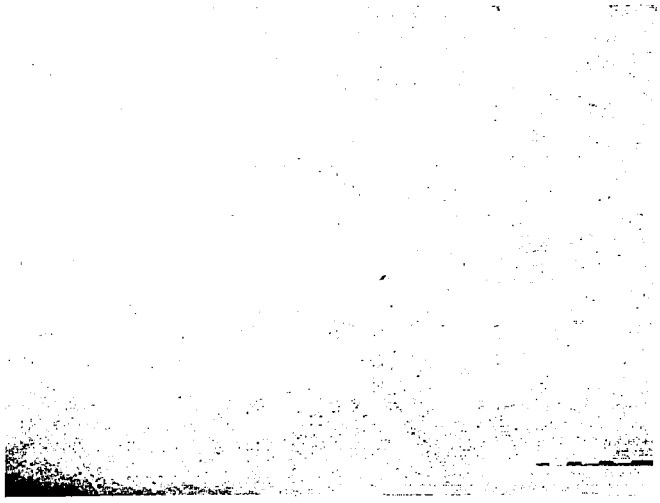

t = 3 min

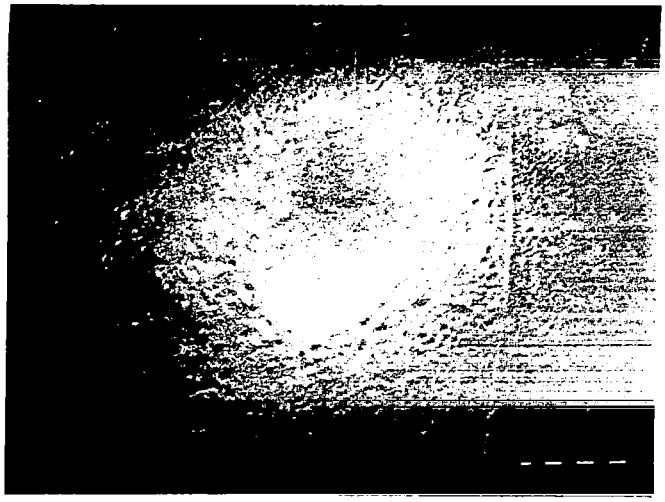

t = 4 min

t = 5 min

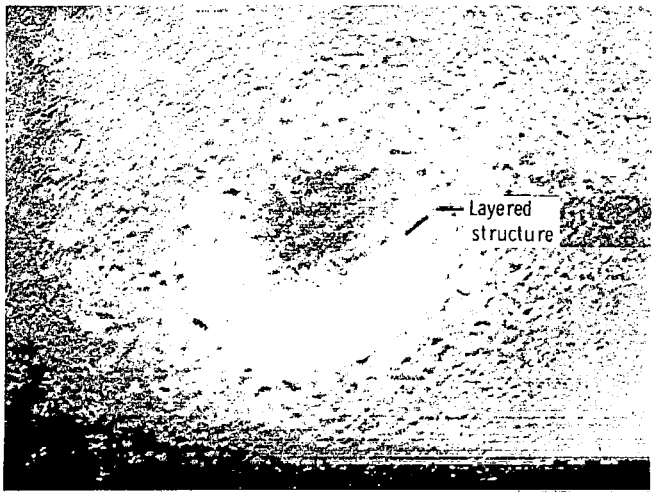

t = 15 min

Figure 6. - Photomicrographs of PTFE surfaces exposed to glass bead impingement at 0.27-megapascal gas pressure as function of time.

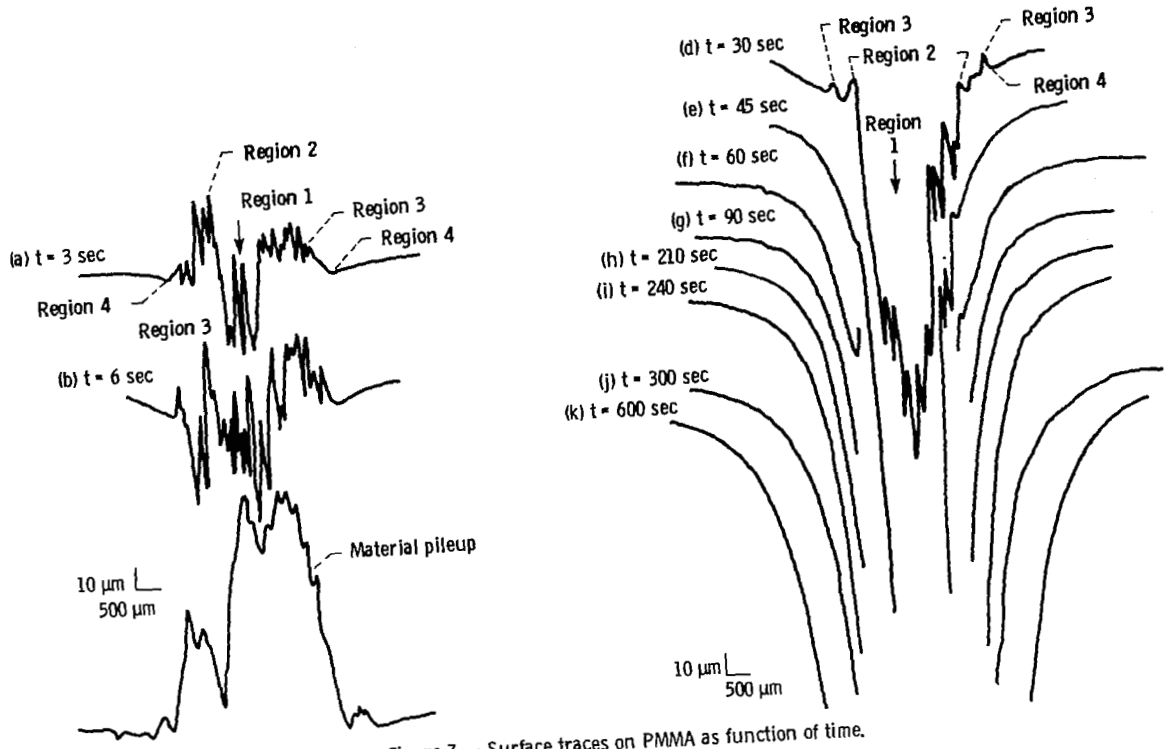

Figure 7. - Surface traces on PMMA as function of time.

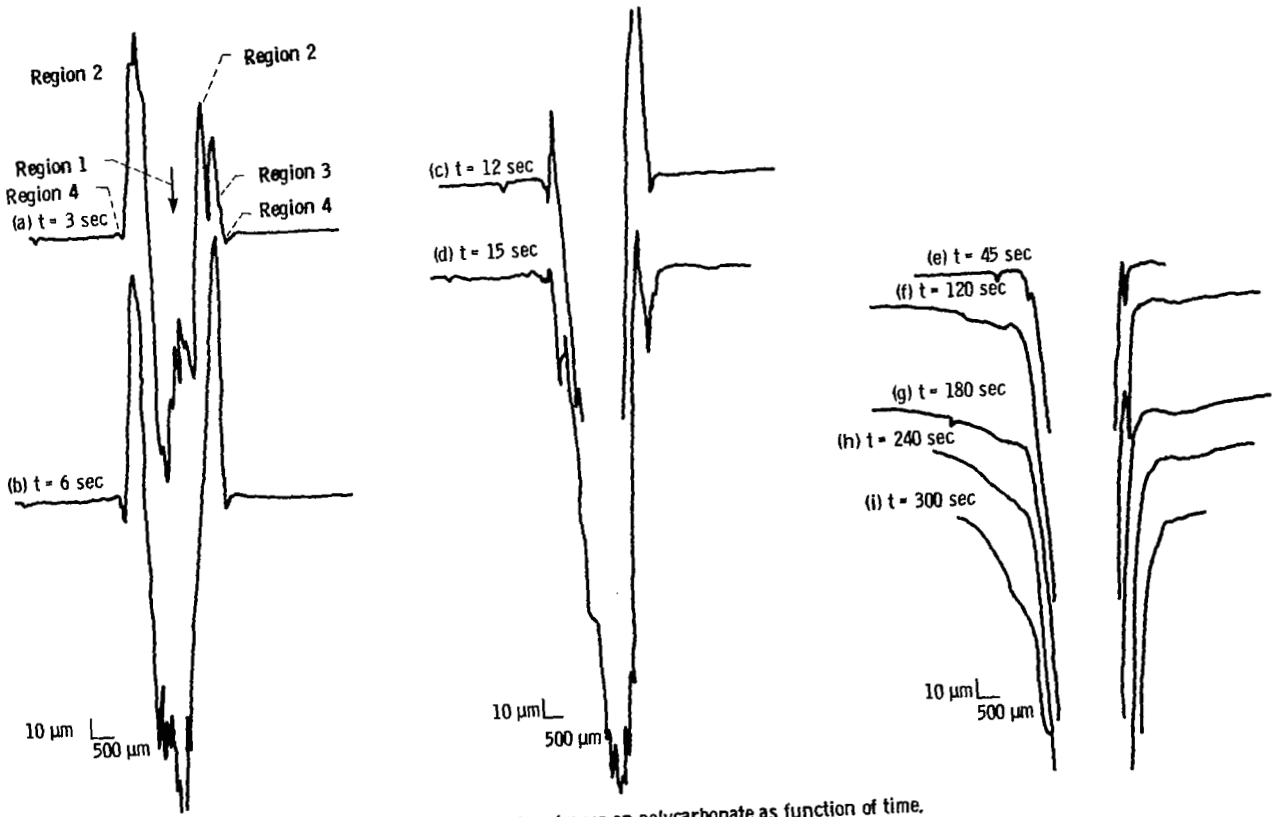

Figure 8. - Surface traces on polycarbonate as function of time.

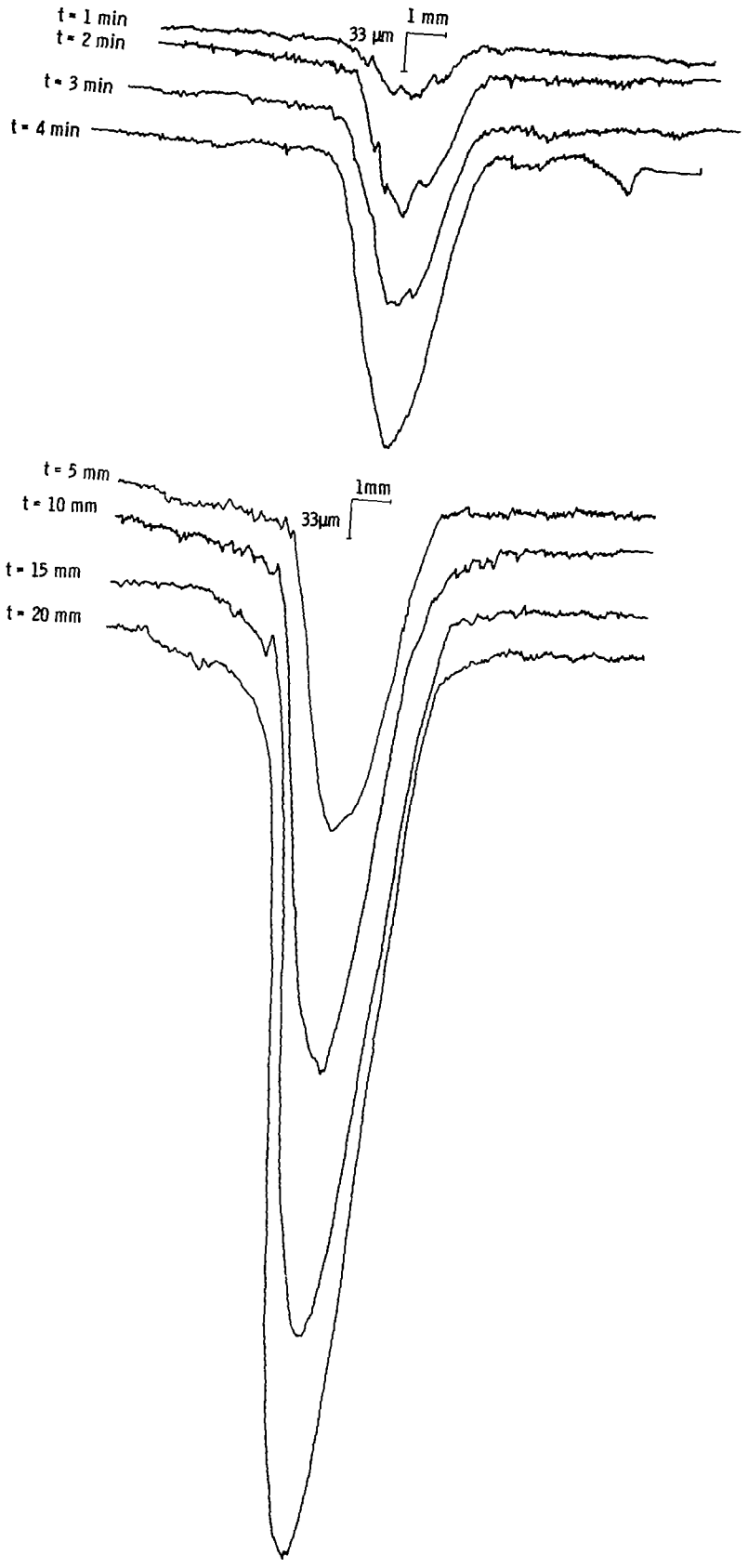

Figure 9. - Surface traces on PTFE as function of time.

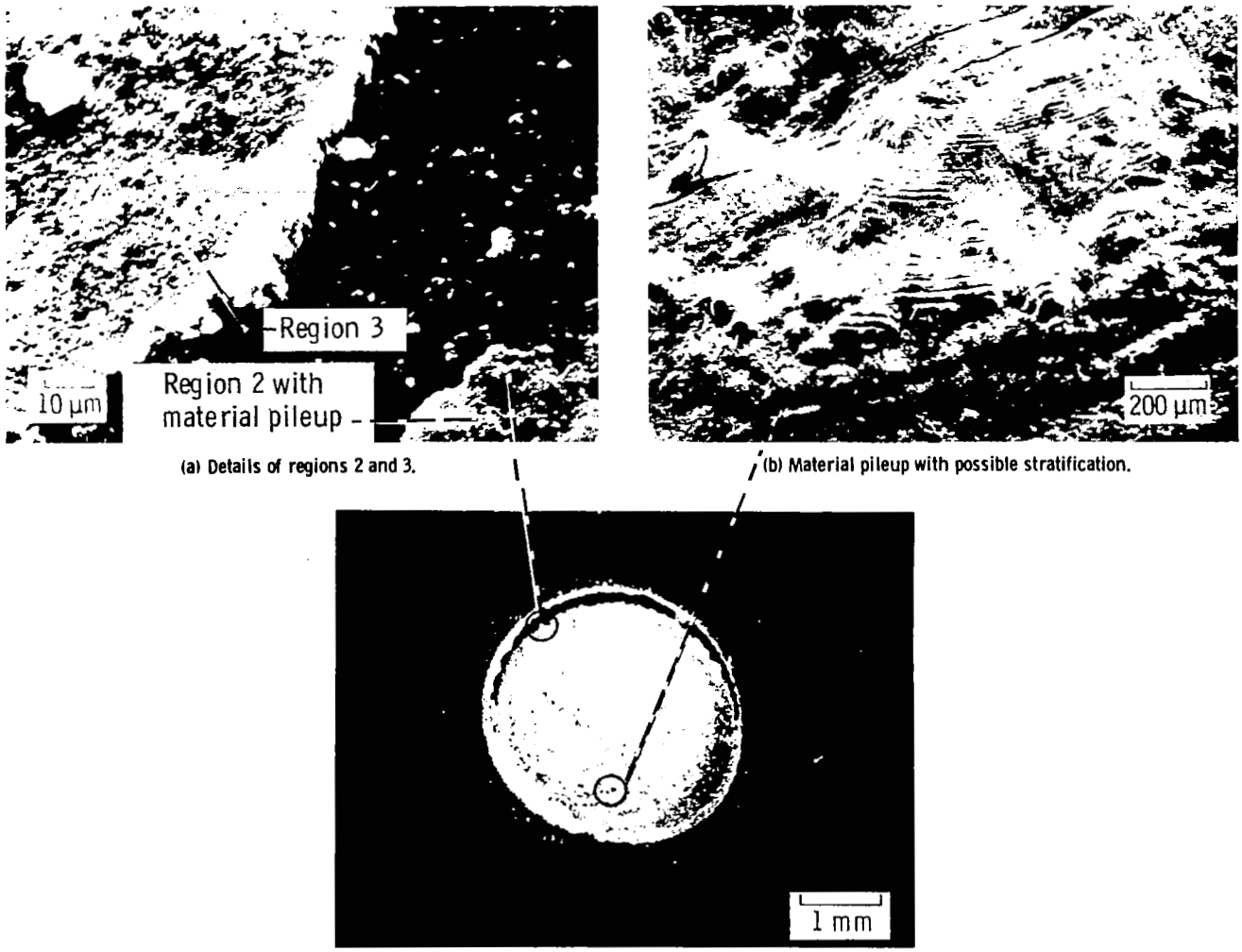

(a) Details of regions 2 and 3.

(b) Material pileup with possible stratification.

(c) 40° tilt photomicrograph of material flow of eroding pit.

Figure 10. - SEM photomicrographs (40° tilt) of PMMA specimen exposed to glass beads for 15 seconds at 0.27-megapascal gas pressure.

As erosion progresses for PMMA, the pit in region 1 deepens and broadens (figs. 4 and 7). Region 2 gradually deepens and disappears. After a 10-minute exposure all regions merge into the main pit. For polycarbonate, regions 3 and 4 are clear at first but gradually disappear with very long exposures (fig. 8). In both cases, at advanced stages of erosion, the pit slopes (region 1) become very smooth (fig. 11). Figure 11 shows SEM micrographs of eroded specimens of PMMA, polycarbonate, and PTFE after 10-minute exposures.

Deep holes are observed for PMMA and polycarbonate. PTFE appears to retain a relatively unstructured damage pattern after 10 minutes (fig. 11(c)). However, after a 15-minute exposure a layered structure is observed along the pit sides (fig. 6, $t = 15$ min).

Erosion-Time Curves

Cumulative erosion-time curves for PMMA, polycarbonate, and PTFE are shown in figures 12 and 13. Table II presents the data for the three plastics at 5-, 10-, 15-, and 20-minute exposures. PMMA erodes rapidly compared with polycarbonate and PTFE (also evident from profiles in figs. 7 to 9). PTFE is observed to be the most resistant of the three thermoplastic polymeric materials. The results in table II and figure 12 show good reproducibility for the erosion process of plastic materials under normal impingement. The scatter of data increased with increased volume loss.

Additional data have been added to the curve for PMMA in figure 12 to show that typical erosion volume loss curves can be divided into different stages. The

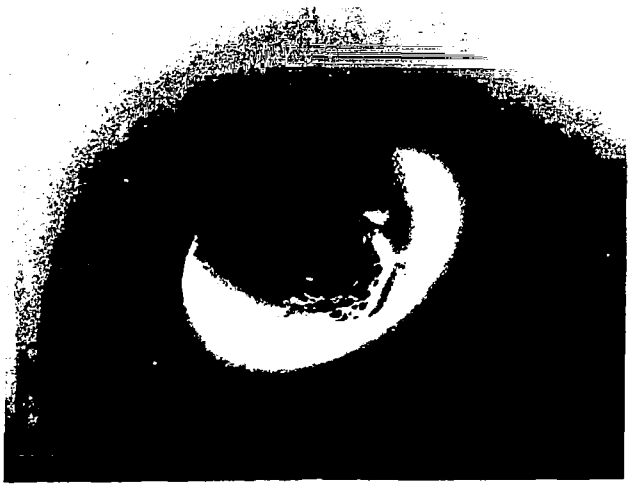

(a) PMMA.

(b) Polycarbonate.

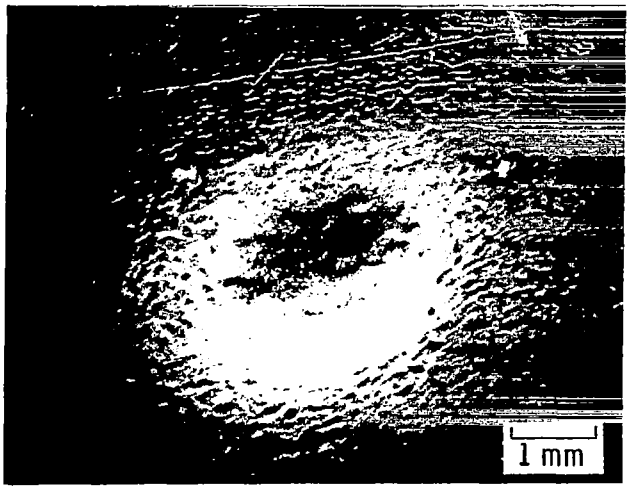

(c) PTFE.

Figure 11. - SEM photomicrographs (40° tilt) of eroded specimens exposed to glass beads at 0.27-megapascal gas pressure for 10 minutes. Corresponding surface profiles shown in figures 7 to 9.

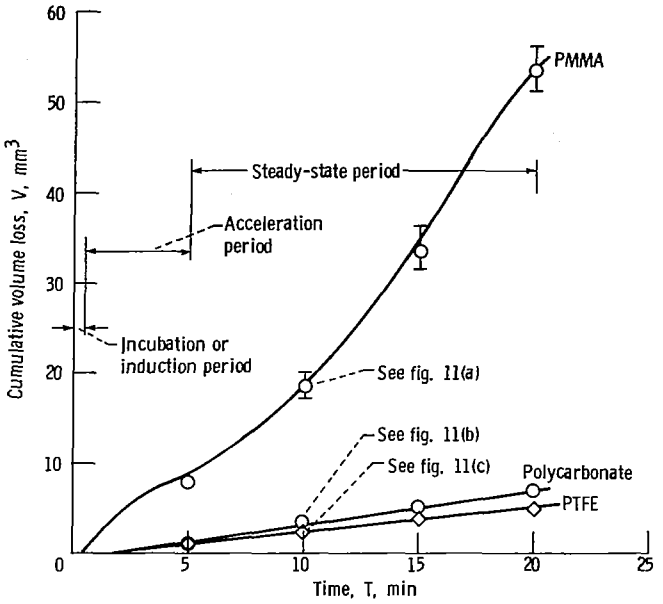

Figure 12. - Cumulative erosion - time curves for plastic materials at 0.27-megapascal gas pressure.

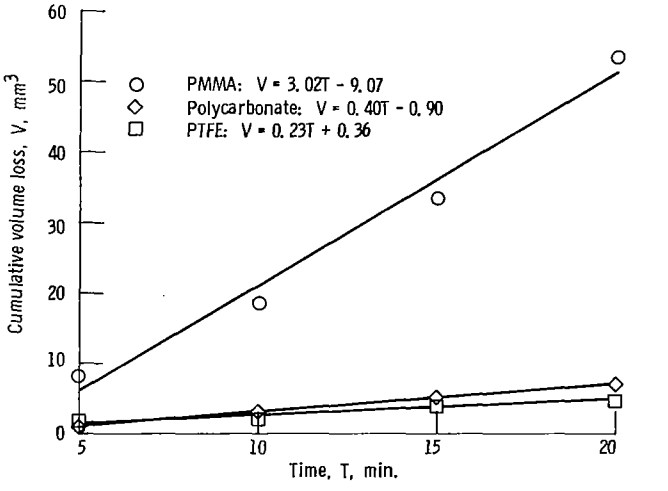

Figure 13. - Least squares fit of data derived from glass bead erosion of plastic materials at 0.27 -megapascal gas pressure.

induction or incubation period exists when there is little or no weight loss. The acceleration period is the time during which the weight loss rate increases rapidly until it reaches a peak. After this there is often a constant or steady-state period, but in these experiments erosion rates increase for PMMA. Analysis of the data (refs. 14, 15, and 17) indicates that erosion rate—time curves on nylon, polypropylene, and polyurethane exhibit incubation (with and without deposition), acceleration, and steady-state periods. Plots of carbon and glass reinforced nylon, however, show incubation, acceleration, peak erosion rate, and deceleration periods. The deceleration period is the time during which the weight loss rate decreases from a peak value.

TABLE II. - SCATTER AND STATISTICAL PARAMETERS OF EXPERIMENTAL DATA

Material	Time, min	Number of specimens tested	Average volume loss, mm^3	Standard deviation	Variance
PMMA	5	8	8.39	0.20	0.03
	10	6	18.89	1.09	.95
	15	4	33.69	1.92	2.77
	20	2	53.80	N/A[a]	N/A
Polycarbonate	5	8	1.10	.32	.09
	10	6	3.04	.22	.04
	15	4	5.19	.10	.008
	20	2	7.03	N/A	N/A
PTFE	5	8	1.37	.10	.009
	10	6	2.83	.19	.03
	15	4	3.91	.12	.01
	20	2	4.85	N/A	N/A

[a]Not applicable, N/A.

In order to compare the volume loss data for these materials on a common basis, figure 13 presents least squares fit straight lines through the average cumulative volume loss data from table II, and linear equations are included to show the approximate slopes and intercepts for the lines drawn through the four data points for each material. The values of the slopes of the lines in cubic millimeters per minute can be used for comparative purposes: PMMA, 3.02; polycarbonate, 0.40; and PTFE, 0.23 cubic millimeter per minute.

Erosion Resistance

Erosion resistance can also be defined as the ratio of the volume of impacting particles to the volume of material removed; the higher the ratio, the higher the erosion resistance. Each material tested was impacted with the same volume of glass beads per unit time (0.98 g/sec). Therefore, approximate erosion resistance numbers for the three materials are PMMA, 20; polycarbonate, 150; and PTFE, 260.

The following discussion on ranking the erosion resistance of the tested materials is based on the properties listed in table I. The erosion resistance varies directly with the ultimate elongation, strain energy, and maximum service temperature; it varies inversely with tensile strength, yield strength, and modulus of elasticity. No single property is clearly dominant in its effect on erosion resistance. It is believed, however, that some combination of high ultimate elongation, impact strength, maximum service temperature, and low modulus of elasticity contributes to high erosion resistance.

Table III presents a summary of erosion results and conditions on elastomeric and plastic materials by different investigators (refs. 2, 3, 7, and 12 to 15). This table shows bulk composite materials, nylon, epoxy, and polypropylene to be less resistant to erosion than the metals tested. Table III also presents the order of erosion resistance of different plastics and related materials and a brief explanation of erosion mechanism and resistance by the various investigators. When PMMA was tested by other investigators (refs. 12, 13, 16, and 19) using entirely different shapes and sizes of abrasive particles and different experimental devices, very low erosion resistance was indicated when compared to other nonmetallic materials (consistent with our results). For elastomers, these investigators found that filled rubber tire tread showed the highest resistance of all nonmetallic materials tested to erosive wear (refs. 12 and 22). Other investigations (ref. 23) have shown that natural and synthetic rubbers exhibit good erosion resistance because of their low modulus of elasticity and that some correlation exists with ultimate resilience (defined as (tensile strength)^2/2(modulus of elasticity)) and with density of materials (ref. 16). From the data in table I, the ultimate resilience does not vary sufficiently to arrive at the same conclusion in the current study. Many more materials with carefully measured properties need to be tested to draw any clear conclusions regarding material property correlations with erosion resistance.

Material Removal Processes

To more thoroughly study features of the material removal process during exposure to glass bead impingement, 500X SEM micrographs were taken of the eroded specimens (fig. 14). Platelets or flakes were observed which looked similar to those observed on aluminum alloy (ref. 24) under identical impingement

TABLE III. - EROSION CHARACTERISTICS OF PLASTIC AND OTHER RELATED MATERIALS TESTED BY VARIOUS INVESTIGATORS USING DIFFERENT DEVICES AND ERODENT PARTICLES

Investigator	Testing device	Nonmetallic material	Abrasive or particles used	Size, μm	Impact velocity, m/sec	Angle of impact, deg	Erosion, cm^3/kg	Mechanism/erosion resistance
Tilly (ref. 2)[a]	Whirling arm erosion rig	Epoxy resin	Quartz	25 55 100 115 140 170 190	128	90	1.27 3.09 4.45 6.31 6.61 6.59 8.71	Resilient plastics exhibit an initial increase in erosion with particle size until the onset of a saturation plateau where erosion is independent of size.
Goodwin et al. (ref. 3)[a]	Whirling arm erosion rig	Fiberglass	Quartz	125 to 150	61 122 146 244	90	1.6 6.3 14.9 39.1	Fiberglass incurs the most erosion, and the other plastics tested (polypropylene and glass reinforced nylon 66) are poorer erosionwise than the metals.
		Glass/nylon			52 76 99 137 183		.2 .4 .9 2.1 3.9	
		Polypropylene			61 76 99 122 137 192 237		.1 .2 .3 .5 .8 1.4 2.5	
Neilson and Gilchrist (ref. 7)	Air stream nozzle method	Tufnol Perspex	Iron grid Iron grid	500 500	(b) (b)	90 90	(c) (d)	For brittle materials, failure appears to be caused by cracking followed by crazing and subsequent spalling of material.
Russel and Lewis (ref. 12)	Air jet impact test	Rubber tire tread Red rubber Lucite Bakelite Graphite	No. 180 grit emery abrasive	---	(e)	60	[f]0.004 [f]36 [f]51 [f]99 [f]250	Rubber tire tread shows by far the least abrasion of any of the materials tested.

[a]Values presented herein calculated from curves presented in reference cited.
[b]Air pressure, 0.17 MPa (gage) (25 psi).
[c]Erosion rate, 3.77 g/50 lb/0.5 min.
[d]Erosion rate, 3.22 g/50 lb/2 min.
[e]Air pressure, 0.51 MPa.
[f]Erosion units, $cm^3/10$ kg.

TABLE III. - Continued.

Investigator	Testing device	Nonmetallic material	Abrasive or particles used	Size, μm	Impact velocity, m/sec	Angle of impact, deg	Erosion, cm^3/kg	Mechanism/erosion resistance
Neilson and Gilchrist (ref. 13)	Air stream nozzle method	Perspex	Al_2O_3	210	128	20 25 30 40 45 50 60 70 80 90	[g]1.6 [g]2.0 [g]2.3 [g]2.8 [g]2.8 [g]2.7 [g]2.5 [g]2.5 [g]2.4 [g]2.4	From the tests on perspex it appears that it is a material of the type where neither cutting wear nor deformation wear predominates. For this material no deposition effects are observed and erosion is detected at small angles of attack.
Tilly (ref. 14)	Air blast erosion rig	Nylon Carbon reinforced nylon Glass reinforced nylon Polypropylene	Quartz	60 to 125	103.6	20 30 45 60 90 20 30 60 90 20 30 45 60 90 20 30 45 90	0.064 .099 .028 .003 -.026 .078 .064 .018 -.021 .066 .079 .025 .005 -.013 .012 .014 .010 -.035	Polypropylene incurs slightly more deposition than the other plastics at 90° (i.e., large incubation period). For the plastics the surface topography is less well defined but there seems to be evidence of grooving in the direction of impact. Typical samples of the nylon chippings are found to be flakes ∿10 μm thick. The fiberglass is found to break into its separate constituents because the glass fibers are broken cleanly with no epoxy attached. The epoxy chippings are in the form of flat flakes (∿20 mm thick). Erosion processes for plastics are not clear. -
Tilly and Sage (ref. 15)[a]	Whirling arm erosion rig	Nylon 30-Percent glass reinforced nylon	Quartz	125 to 150	53.3 152.4 243.8 289.6 50.3 74.7 100.6 134.1 213.3	90	0.22 .68 3.10 3.80 .20 .45 .85 2.57 4.57	Reinforcement of plastics can either improve or worsen their erosion resistance properties, depending on the nature of reinforcing materials. Composite materials are generally rather poor. Nylon, which is one of the best avail-

[a]Values presented herein calculated from curves presented in reference cited.
[g]Erosion units, g/kg.

TABLE III. - Concluded.

Investigator	Testing device	Nonmetallic material	Abrasive or particles used	Size, μm	Impact velocity, m/sec	Angle of impact, deg	Erosion, cm^3/kg	Mechanism/erosion resistance
Tilly and Sage (ref. 15)[a]	Whirling arm erosion rig	25-Percent carbon reinforced nylon	Quartz	125 to 150	57.9 94.5 121.9 243.8 295.7 342.9	90	0.24 .43 1.20 5.89 9.10 12.88	able plastics, deteriorates by about 4 to 1 when reinforced by glass or carbon fibers. On the other hand, a commercial variety of epoxy resin is one of the poorest materials erosionwise. A very substantial improvement is obtained with steel powder reinforcement, although it is still ten times worse than the solid steel. Unfortunately, at present there are insufficient data to draw any generalized conclusions on the behavior of composites.
		Epoxy resin			61.0 91.4 121.9 160.0 196.6 304.8		1.15 8.51 12.50 19.95 70.85 90.11	
		70-Percent glass reinforced epoxy			61.0 121.9 144.8 243.8		1.47 6.91 13.80 35.49	
		80-Percent steel reinforced epoxy			59.4 61.0 121.9 182.9 253.0		.35 .28 1.68 3.89 7.08	
		Nylon		17 25 37 50 70 98 135 200 200	243.8		.35 .34 1.19 1.90 2.44 2.84 3.12 2.91 2.58	
		Type 66 nylon Polypropylene Glass reinforced nylon Fiberglass Polyurethane		125 to 150	244 128		2.3 3.1 7.0 7.0 53.0	
Present study	Sand blasting device	PMMA Polycarbonate PTFE	Glass beads Glass beads Glass beads	20 20 20	72 72 72	90 90 90	0.045 .006 .004	See Material Removal Processes section.

[a]Values presented herein calculated from curves presented in reference cited.

conditions. However, on the aluminum alloy flakes, random impact impressions were noticed which were not observed on the plastic material flakes.

Tilly (ref. 14) has also reported observations of flakes on nylon, fiberglass, and epoxy resin surfaces due to angular particle impingement. Flakes were also observed by Evans and Lancaster for sliding of polyphenylene oxide and polyacetal in n-hexane and n-propanol against stainless steel (ref. 25); by Shen and Dumbleton for dry sliding of polyoxymethylene against stainless steel (ref. 26), and by Shallamach for abrasion of particles and pins against different types of filled and unfilled rubber (refs. 22, 27, and 28). The flakes observed in the present investigation are believed to form due to repeated direct impact and deformation followed by shear and fatigue resulting in complete removal during outflow of particles. The extent of heat distortion and melting, which may play an important role in this process, is unknown at present, but it is believed to be more extensive at the bottom of the crater than at the sides.

It has also been observed from the literature that plastic and elastomeric materials such as polypropylene, nylon, PMMA, natural rubber, and Vulkallan B (refs. 2, 13, 14, and 23) behave as either brittle or ductile materials depending on the angle of impingement (table III). Maximum erosion rates have been observed at angles between 15° and 35°, and cutting wear is indicated by sharp faceted surfaces. For higher incidence angles (including normal), the damage patterns (including the observation of flakes) appear similar to those for ductile metals. This is indicative of the predominance of wear due to deformation as opposed to cutting.

In our studies cutting wear (ref. 29) appears to be absent for all three plastic materials. This was expected as most of the spherical glass beads were not broken even after impact (ref. 24), and the material was worn due to deformation by repeated impact and eventual fatigue rather than by cutting the surface.

For PTFE the flakes appear thinner than those for the other two materials (fig. 14). Thin flakes were also reported for the more resistant nylon in reference 14, and large flat flakes were reported in reference 15 for heavily eroded epoxy resin. Hence, thinner flake formation may be related to higher erosion resistance.

Summary of Results

Studies of glass bead impingement at normal incidence on polymethyl methacrylate (PMMA), polycarbonate, and polytetrafluoroethylene (PTFE) have been conducted. Argon was used as the driving gas at a pressure of 0.27 megapascal (gage). Changes in surface morphology, material removal with time, erosion resistance, and surface chemistry were studied.

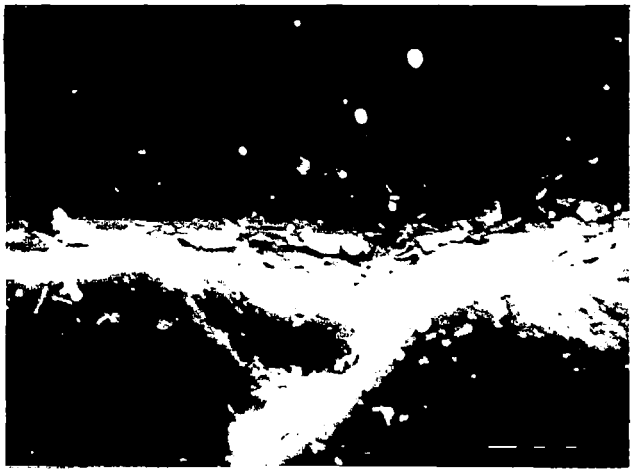

(a) PMMA.

(b) Polycarbonate.

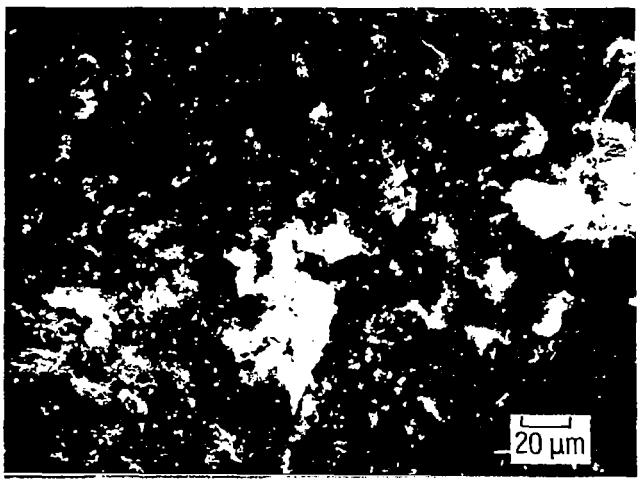

(c) PTFE.

Figure 14. - SEM photomicrographs (40° tilt) of eroded specimens showing material dislodging process. Specimens exposed to glass beads at 0.27-megapascal gas pressure for 10 minutes.

1. Initially, a buildup of material composed of a combination of target materials and erodent particles was observed around the pit for all materials during the early stages of damage. The maximum was observed on polycarbonate and the least for PTFE. After further exposure material buildup and any other features on the surface disappeared as the main pit developed.

2. Some evidence for melting at the pit centers was observed as was subsequent solidification on the sides.

3. PTFE was found to be the most resistant to erosion and PMMA the least resistant.

4. A dimensionless parameter for erosion resistance, which is the ratio of the volume of erodant particles to the material lost, resulted in numbers of 20 for PMMA, 150 for polycarbonate, and 260 for PTFE.

5. A combination of high ultimate elongation, strain energy, maximum service temperature, and low modulus of elasticity appears to be consistent with high erosion resistance.

6. SEM micrographs show flake-type debris in the eroding pits of the thermoplastic materials. Material loss is believed to be due primarily to the breakup and removal of these flakes. Smaller, thinner flake formation appears to correlate with higer erosion resistance.

Lewis Research Center
National Aeronautics and Space Administration
Cleveland, Ohio, January 4, 1983

References

1. Sage, W.; and Tilly, G. P.: The Significance of Particle Size in Sand Erosion of Small Gas Turbines. J. R. Aeronaut. Soc., vol. 73, May 1969, pp. 427–428.
2. Tilly, G. P.: Sand Erosion of Metals and Plastics: A Brief Review. Wear, vol. 14, 1969, pp. 241–248.
3. Goodwin, J. E.; Sage, W.; and Tilly, G. P.: Study of Erosion by Solid Particles. Proc. Inst. Mech. Eng., vol. 184, no. 15, Part 1, 1969–70, pp. 279–292.
4. Williams, J. H., Jr.; and Lau, E. K.: Solid Particle Erosion of Graphite-Epoxy Composites. Wear, vol. 29, no. 2, Aug. 1974, pp. 219–230.
5. Schmitt, G. F., Jr.: Impact Erosion—A Serious Environmental Threat to Aircraft and Missiles. ASME Paper 75-ENAS-45, July 1975.
6. Hibbert, W. A.: Helicopter Trials Over Sand and Sea. J. R. Aeronaut. Soc., vol. 69, no. 659, Nov. 1965, pp. 769–776.
7. Neilson, J. H.; and Gilchrist, A.: An Experimental Investigation into Aspects of Erosion in Rocket Motor Tail Nozzles. Wear, vol. 11, 1968, pp. 123–143.
8. Hoenig, S. A.: Meteoric Dust Erosion Problem and Its Effect on the Earth Satellite. Aeronaut. Eng. Rev., vol. 16, no. 7, July 1957, pp. 37–40.
9. Tilly, G. P.: Erosion by Impact of Solid Particles. Treatise on Materials Science and Technology, vol. 13, D. Scott, ed., Academic Press, 1979, pp. 287–319.
10. Schmitt, G. F., Jr.: Liquid and Solid Particle Impact Erosion. Wear Control Handbook, M. B. Peterson and W. O. Winer, eds., American Society of Mechanical Engineers, 1980, pp. 231–282.
11. Adler, W. F.: Assessment of the State of Knowledge Pertaining to Solid Particle Erosion. Rept. ETI CR 79-680, U.S. Army Research Office, 1979. (AD-A073034.)
12. Russel, A. S.; and Lewis, J. E.: Abrasive Characteristics of Alumina Particles. Ind. Eng. Chem., vol. 46, no. 6, June 1954, pp. 1305–1310.
13. Neilson, J. H.; and Gilchrist, A.: Erosion by a Stream of Solid Particles. Wear, vol. 11, 1968, pp. 111–122.
14. Tilly, G. P.: Erosion Caused by Airborne Particles. Wear, vol. 14, 1969, pp. 63–79.
15. Tilly, G. P.; and Sage, W.: The Interaction of Particle and Material Behaviour in Erosion Processes. Wear, vol. 16, 1970, pp. 447–465.
16. Kayser, W.: Erosion by Solid Bodies. Proceedings of the Second Meersburg Conference on Rain Erosion and Allied Phenomena, vol. 2, A. A. Fyall and R. B. King, eds., Royal Aircraft Establishment, Farnborough, England, 1967, pp. 427–447.
17. Tilly, G. P.; and Sage, W.: A Study of the Behavior of Particles and Materials in Erosion Processes. ASME Paper No. 69—WA/Met-6, Nov. 1969.
18. Behrendt, A.: Sand Erosion of Dome and Window Materials. International Conference on Rain Erosion and Associated Phenomena. Royal Aircraft Establishment, Farnborough, England, 1975, pp. 845–861.
19. Soderberg, S.; et al.: Erosion Classification of Materials Using a Centrifugal Erosion Tester. Tribol. Int., vol. 14, no. 6, Dec. 1981, pp. 333–343.
20. Zahavi, J.; and Schmitt, G. F., Jr.: Solid Particle Erosion of Polymeric Coatings. Wear, vol. 71, no. 1, Sept. 1981, pp. 191–210.
21. Weast, R. C., ed.: CRC Handbook of Chemistry and Physics. 55th. ed. CRC Press, Inc., 1974, pp. C-735 to C-742.
22. Schallamach, A.: On the Abrasion of Rubber. Proc. Phys. Soc., London, Sect. B, vol. 67, part 12, Dec. 1954, pp. 883–891.
23. Eyre, T. S.: Wear Characteristics of Metals. Tribol. Int., vol. 9, Oct. 1976, pp. 203–212.
24. Rao, P. Veerabhadra; Young, S. G.; and Buckley, D. H.: Morphology of Ductile Metals Eroded by a Jet of Spherical Particles Impinging at Normal Incidence. Wear, vol. 85, no. 2, April 1983.
25. Evans, D. C.; and Lancaster, J. K.: The Wear of Polymers. Treatise on Materials Science and Technology, D. Scott, ed., vol. 13, Academic Press, 1979, pp. 85–139.
26. Shen, C.; and Dumbleton, J. H.: The Friction and Wear Behavior of Polyoxymethylene in Connection with Joint Replacement. Wear, vol. 38, 1976, pp. 291–303.

ERRATA

NASA Technical Paper 2161

SOLID SPHERICAL GLASS PARTICLE IMPINGEMENT STUDIES OF PLASTIC MATERIALS

P. Veerabhadra Rao, Stanley G. Young, and
Donald H. Buckley
April 1983

Page 16: The following references should be added:

27. Schallamach, A.: Abrasion of Rubber by a Needle. Polym. Sci., vol. 9, no. 5, Nov. 1952, pp. 385–404.
28. Schallamach, A.: Friction and Abrasion of Rubber. Wear, vol. 1, 1957/1958, pp. 384–417.
29. Hutchings, I. M.: Mechanisms of the Erosion of Metals by Solid Particles. Erosion: Prevention and Useful Applications, W. F. Adler, ed., ASTM STP 664, American Society for Testing and Materials, 1979, pp. 59–76.

Date issued: June 1983

1. Report No.	2. Government Accession No.	3. Recipient's Catalog No.
NASA TP-2161		

4. Title and Subtitle	5. Report Date
SOLID SPHERICAL GLASS PARTICLE IMPINGEMENT STUDIES OF PLASTIC MATERIALS	April 1983
	6. Performing Organization Code 505-32-42

7. Author(s)	8. Performing Organization Report No.
P. Veerabhadra Rao, Stanley G. Young, and Donald H. Buckley	E-1122
	10. Work Unit No.

9. Performing Organization Name and Address	11. Contract or Grant No.
National Aeronautics and Space Administration Lewis Research Center Cleveland, Ohio 44135	
	13. Type of Report and Period Covered
12. Sponsoring Agency Name and Address	Technical Paper
National Aeronautics and Space Administration Washington, D.C. 20546	14. Sponsoring Agency Code

15. Supplementary Notes

P. Veerabhadra Rao, National Research Council - NASA Research Associate; Stanley G. Young and Donald H. Buckley, Lewis Research Center.

16. Abstract

Erosion experiments on polymethyl methacrylate (PMMA), polycarbonate, and polytetrafluoroethylene (PTFE) were conducted with spherical glass beads impacting at normal incidence. Optical and scanning electron microscopic studies and surface profile measurements were made on specimens at predetermined test intervals. During the initial stage of damage to PMMA and polycarbonate, material expands or builds up above the original surface. However, this buildup disappears as testing progresses. Little or no buildup was observed on PTFE. PTFE is observed to be the most resistant material to erosion and PMMA the least. At low-impact pressures, material removal mechanisms are believed to be similar to those for metallic materials. However, at higher pressures, surface melting is indicated at the center of impact. Deformation and fatigue appear to play major roles in the material removal process with possible melting or softening.

17. Key Words (Suggested by Author(s))	18. Distribution Statement
Wear; Erosion; Impingement; Morphology; Thermoplastics; Erosion resistance; Glass bead impact	Unclassified - unlimited STAR Category 27

19. Security Classif. (of this report)	20. Security Classif. (of this page)	21. No. of Pages	22. Price*
Unclassified	Unclassified	18	A01

* For sale by the National Technical Information Service, Springfield, Virginia 22161 NASA-Langley, 1983

National Aeronautics and
Space Administration

Washington, D.C.
20546

Official Business
Penalty for Private Use, $300

THIRD-CLASS BULK RATE

Postage and Fees Paid
National Aeronautics and
Space Administration
NASA-451

U.S.MAIL

2 1 1U,C, 830428 S00903DS
DEPT OF THE AIR FORCE
AF WEAPONS LABORATORY
ATTN: TECHNICAL LIBRARY (SUL)
KIRTLAND AFB NM 87117

NASA

POSTMASTER: If Undeliverable (Section 158
Postal Manual) Do Not Return